AIAA 80-0231R

Recent Development of a Jet-Diffuser Ejector

Morton Alperin* and Jiunn-Jenq Wu†
Flight Dynamics Research Corporation, Van Nuys, Calif.

Although the concept of ejector momentum augmentation has been discussed in technical literature numerous times during the past sixty years, the practical application of such devices to aircraft design has never been accomplished. The difficulties encountered in aircraft applications are related to the popular concepts (or misconceptions) that the processes of mixing and diffusion are required to proceed to completion within the solid surfaces of the ejector, which generally result in long ejectors with poor performance. Thrust augmenting ejectors in which the processes of mixing and diffusion are carried out, in part, in a region downstream of the solid surfaces of the ejector (in a jet diffuser) have recently been successfully operated in the Flight Dynamics Research Corporation (FDRC) Laboratory. A jet sheet surrounding the periphery of a widely diverging diffuser prevents separation and if properly designed, forms a gaseous, curved surface downstream of the solid surface, to provide additional, effective diffuser area ratio and additional length for mixing of primary and induced flows. Three-dimensional potential flow methods were recently utilized to provide a design technique for achievement of a large reduction in the length requirement for the associated solid surface. Primary nozzle design, involving consideration of aircraft integration, internal and external losses, and performance trade-offs, have been used to further reduce the volume required by these jet-diffuser ejectors, resulting in thrust augmentation in excess of 2, and an overall length of about two and one-half times the throat width.

Nomenclature

A_2 = cross-section area of ejector throat
a_∞ = primary jet area when mass flow is expanded isentropically to ambient pressure
p,P = gage pressure
s = curvilinear distance along streamline
s_∞ = diffuser jet area when mass flow is expanded isentropically to ambient pressure
t = thickness of jet slot
V = (u,v,w) velocity vector
x,y,z = coordinates
X_2 = throat width of ejector
α_∞ = (A_2/a_∞), inlet area ratio
β = angle of diffuser surface to thrust direction
Γ = circulation
δ = diffuser area ratio
ϕ = thrust augmentation = ejector net thrust/net thrust of free reference jet (reference jet has same mass flow as that of the ejector's energized flow, and stagnation conditions identical to those of the plenum of the ejector)
ϕ' = thrust augmentation for tube nozzles
ξ,η,θ = position and orientation of detached primary nozzles
ω = induced flow angle, defined similar to θ

Subscripts

CL = center of ejector throat
d = diffuser jet
e = end of diffuser surface
0 = stagnation, or starting point for diffuser surface calculation (at the diffuser jet slot)
p = primary jet
∞ = ambient condition

Presented as Paper 80-0231 at the AIAA 18th Aerospace Sciences Meeting, Pasadena, Calif., Jan. 14-16, 1980; submitted Jan. 16, 1980; revision received July 1, 1980.

*Technical Director. Member AIAA.
†Research Director.

I. Background

THRUST augmenting ejectors are solid or fluid ducts which accept energized (primary) fluid and a quantity of ambient fluid which is induced to flow through the ejector as a result of a mixing process which occurs within the ejector. In general, the mixing process consists of an exchange of kinetic and thermal energy between the primary and induced flows, ending in a flow in which the enthalpy and velocity are nonuniformly distributed over any given cross section, unless the length of the ejector in the flow direction is extremely large. In addition, analyses of the flow through a conventional V/STOL ejector having an accelerating inlet and a diffusing outlet (recent theoretical discovery indicates that there are other types of ejectors which may not require a diffuser[1]) have indicated that even with complete mixing, high performance requires large area ratio diffusers which, if separation is to be avoided, must diverge slowly. Therefore conventional ejectors require long lengths of solid surfaces in the flow direction, a fact which leads to the popular concept (or misconception) that ejectors must be large in order to achieve high thrust augmentation.

Attempts to reduce the length required for mixing of primary and induced flows have until recently been restricted to the use of multiple injection jets with various shapes and/or injection of curved flows to create large vortices, which are known to accelerate the mixing process. Such techniques are frequently accompanied by a reduction of the primary nozzle efficiency and a large momentum degradation of the induced flow, and therefore result in little improved performance. Attempts to reduce the length of large area ratio diffusers have consisted primarily of the use of high velocity blowing jets, immediately upstream of the point of separation of rapidly diverging solid surfaces. Some success has been achieved by this technique, but the gain in ejector performance has been small since the momentum required by the blowing jets must be charged against the injected momentum, in the evaluation of the overall thrust augmentation. The mixing process cannot be accelerated except at the expense of the momentum of the primary or the induced flow or both, and a long diffuser duct introduces excessive frictional drag. Recent research[2] reveals that enlargement of the effective diffuser area ratio can compensate for incomplete mixing. Therefore it is appropriate to design high performance

thrusting ejectors (with accelerating inlets and diffusing outlets) having short, large area ratio diffusers, and accepting incomplete mixing at the exit of the ejector structure. Such designs are more easily integrated into aircraft configurations, and provide high performance.

A means for achieving large reductions in the solid length of a large area ratio diffuser, and for provision of a long region downstream of the end of the solid surfaces, for effective mixing, was developed under the Small Tactical Aerial Mobility Platform (STAMP) program.[3] The technique utilized in the STAMP ejector consisted of the injection of a continuous blowing jet (jet-diffuser), completely surrounding the periphery of the diffuser. Injection of this diffuser jet immediately upstream of any possible separation, and then rapidly diverging the solid surface downstream of the diffuser jet, to achieve solid diffuser area ratios in excess of 3.0, proved very successful, as reported in Ref. 3. That ejector displayed thrust augmentation in excess of 2.0, with a solid diffuser length about equal to its throat width. The duct structure of this ejector consists basically of two identical cylindrical surfaces, separated by a distance equal to their radius, as illustrated in Fig. 1. This ejector, designated AJDE (Alperin Jet-Diffuser Ejector) by the U.S. Navy, performs several important functions, and has several limitations.

Although jet-diffusion performs its designated function of providing large diffuser area ratios and extending the diffusion process beyond the end of the solid surface, the three-dimensional effects at the ends of the rectangular ejector limit its performance. Attempts to diverge these ends as little as 5 deg during the STAMP Program resulted in local flow separation and severe performance degradation. With flat, nondiverging ends, the diffuser jet sheet cannot sustain any pressure differential and the flow pattern collapsed before reaching the end of the plate and seriously degraded the effective diffuser area ratio in a manner similar to the effect caused by separation in a solid diffuser. The addition of end plates extending beyond the solid, diverging sides of the diffuser, provided a means for avoiding this problem and as shown on Fig. 1, where the thrust augmentation (ratio of ejector thrust to the thrust of a free jet whose mass flow is equal to that of the energized flow into the ejector and whose stagnation conditions are equal to those of the ejector's plenum conditions) improved rapidly with increasing end plate size.

The ability of jet diffusion to maintain subambient pressure downstream of the solid, diverging surface of the diffuser is illustrated in Fig. 2 where, as shown by the isobars, the diffusion region extends far beyond the diverging ends of the solid diffuser surface. As shown, these data were acquired with the use of a large end plate extending to 27 cm beyond the diverging ends, thus avoiding the collapse of the flow pattern, which would have occurred if the end plates were removed.

Using the potential flow theory, a pair of two-dimensional counter rotating vortices was assumed to have a strength and position such as to provide a streamline corresponding to the cylindrical surface of the jet diffuser ejector duct. The pressure distribution resulting from this vortex pair is compared to that measured experimentally in the ejector. The excellent agreement between the theory and the experiment, as illustrated in Fig. 3, leads to the use of potential flow theory for prediction of the flow in the ejector, despite the presence of viscous flow phenomena such as mixing and skin friction. The methods of potential flow may even be assumed to be appropriate for use in ejector design when high pressure gas is injected at the primary jet, particularly, as in the case of the type of ejector under consideration, when the mixed flow is subsonic and the optimal performance occurs with subsonic induced flow. For further details see Ref. 1.

II. Three-Dimensional Jet Diffuser

An investigation was undertaken to derive a potential flow shape for the solid diffuser, under the assumption that flow separation is primarily due to excessive adverse pressure gradients. By the method of potential flow, shapes and corresponding local pressure gradients could be determined,

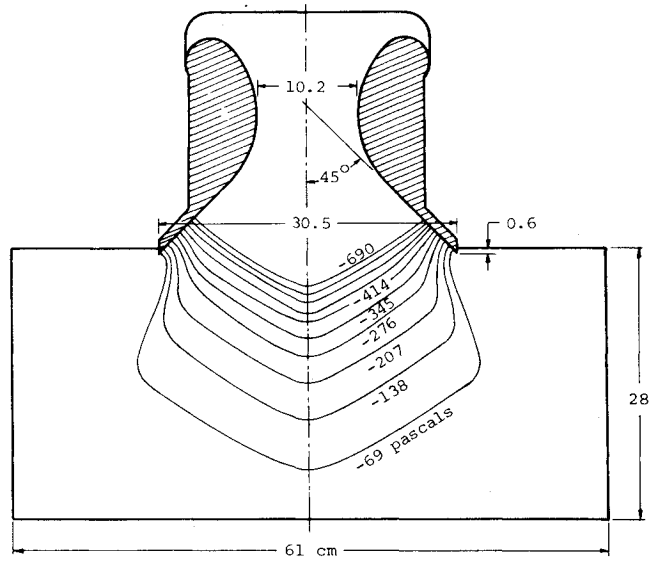

Fig. 2 Isobars on end plate of STAMP ejector.

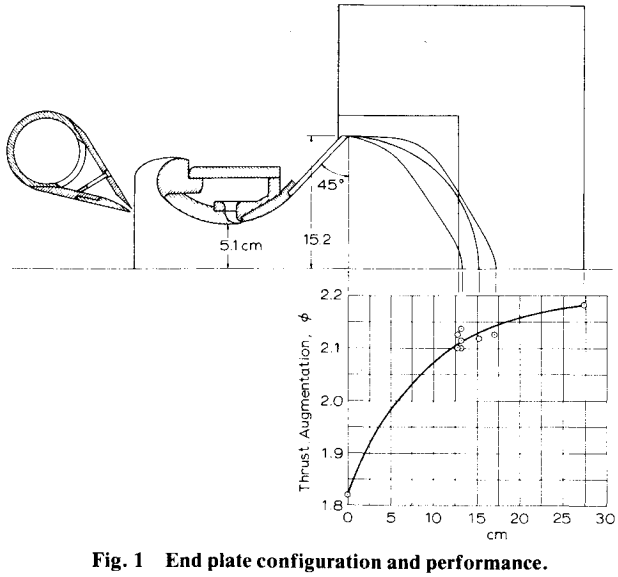

Fig. 1 End plate configuration and performance.

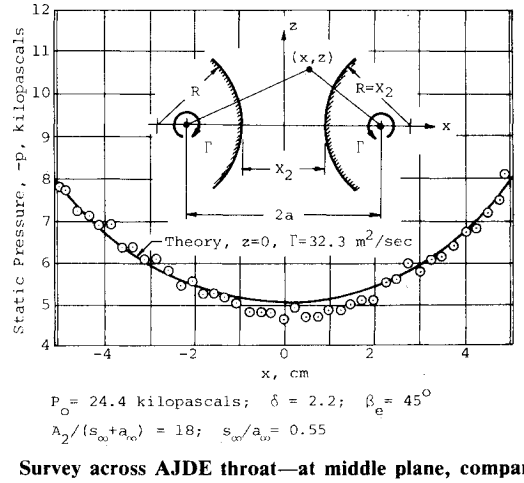

Fig. 3 Survey across AJDE throat—at middle plane, compared to potential flow theory.

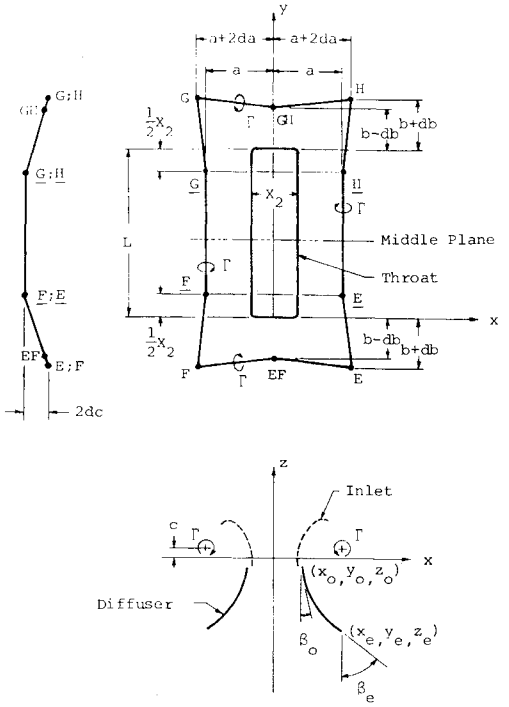

Fig. 4 Coordinate system.

and three-dimensional diffuser shapes could be constructed for a series of diffusers having various maximum pressure gradients. The acceptable maximum pressure gradient for a given diffuser jet configuration was determined from the STAMP experiments.

The potential flow method assumed a closed distribution of constant strength vortices whose location and size were chosen in a manner which produced a streamline which matched the geometric properties of the middle plane of the AJDE. Various vortex distribution shapes were utilized to calculate the diffuser shape and local pressure gradients. The generalized vortex distribution is shown in Fig. 4. This generalized ring vortex system consists of six independent parameters: *a, b, c, da, db,* and *dc*. Since there are only two geometric requirements on the middle plane of the ejector:

1) flow angle (β_0) at the diffuser jet location (x_0, y_0, z_0) and

2) diffuser exit angle (β_e) at a specified diffuser area ratio ($2x_e/X_2$), only four free parameters can be varied for numerical experiment. The four independent parameters chosen for this study are *a, da, db,* and *dc,* while *a* and *c* are determined by the middle plane requirements. Using this general formulation, the local velocity vector and pressure can be evaluated in the following manner.

The velocity vector V resulting from a vortex element between points A and B (Fig. 5) can be evaluated at any point (P) by the relationship

$$V=(\Gamma/4\pi h)(\cos\theta_1+\cos\theta_2)\boldsymbol{n}$$

where $\boldsymbol{n}$ is the unit vector normal to the plane *ABPA*. The streamline shape can then be determined from a knowledge of the velocity field since by definition of a streamline,

$$dx{:}dy{:}dz = u{:}v{:}w$$

and therefore

$$\frac{dx}{dz}=\frac{u}{w}$$

$$\frac{dy}{dz}=\frac{v}{w}$$

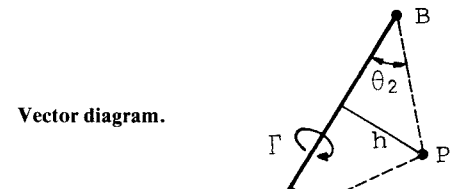

Fig. 5 Vector diagram.

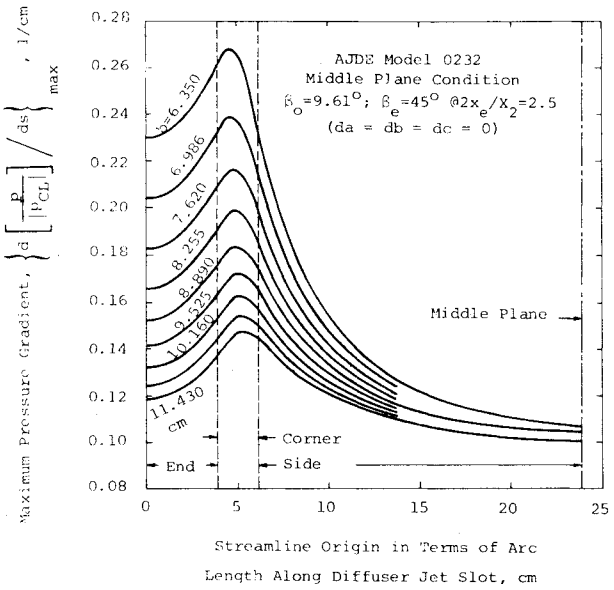

Fig. 6 Maximum pressure gradient for diffuser represented by ring vortices.

and

$$x=x_0+\int_{z_0}^{z}\frac{u}{w}\,dz$$

$$y=y_0+\int_{z_0}^{z}\frac{v}{w}\,dz$$

The pressure can then be determined from the velocity field by application of Bernoulli's equation

$$p=-(\rho/2)\,|V|^2$$

for an ejector which is stationary with respect to the undisturbed flow.

It is important to note that since all gage pressures (and the ability of the diffuser jet to prevent separation) are approximately proportional to the gage plenum pressure, it is possible to use dimensionless pressures in terms of the pressure at the ejector's center (p_{CL}).

Initially, the simplest case of a rectangular planar ring vortex where $da=db=dc=0$, was utilized to determine the local dimensionless pressure p/p_{CL}, and the local pressure gradients for streamlines originating at various peripheral locations at the diffuser jet slot, and continuing until their slope reached a 45-deg angle (which is the diffuser exit angle of the STAMP ejector) with respect to the thrust axis. The distribution of maximum pressure gradient determined by this calculation is presented in Fig. 6 for various values of *b*. As indicated, the maximum pressure gradient is located at the corners of the ejector and its magnitude decreases with increasing values of *b*. Since the maximum pressure gradient corresponding to $b=10.160$ cm is closely equivalent to the theoretical maximum pressure gradient of a two-dimensional vortex pair which produces a streamline corresponding to the shape of the AJDE, and since larger values of *b* result in

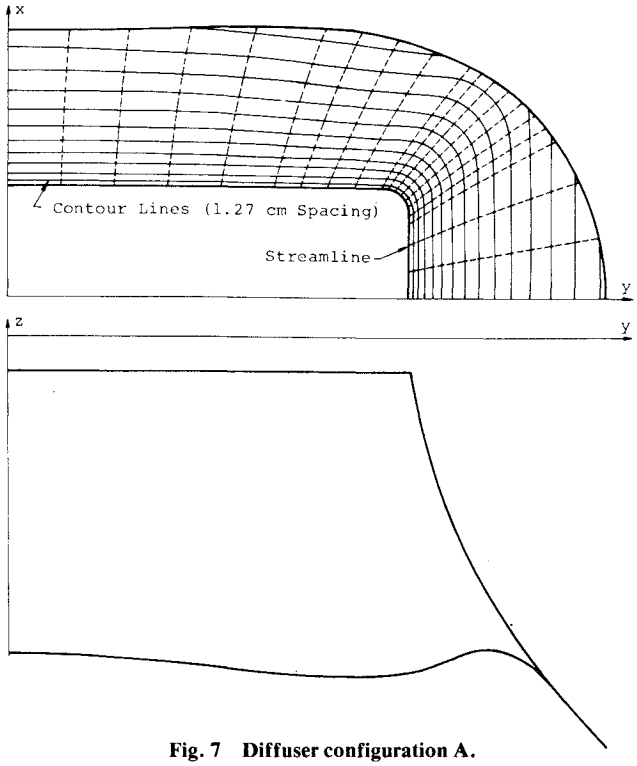

Fig. 7 Diffuser configuration A.

longer diffusers, a diffuser shape derived from $b = 10.160$ cm (configuration A) was chosen for fabrication. Contour lines spaced at 1.27 cm and streamlines for this configuration are shown plotted in Fig. 7.

The ejector was tested with configuration A diffuser using air compressed to 24.1-kPa gage as the energy source. Under these conditions, the thrust augmentation reached a value of 2.01 at an area ratio $[A_2/(s_\infty + a_\infty)]$ of 20.6 without the use of the flat end plates required by the AJDE. However, large peripheral gradients existed in the diffuser and appeared to limit the proper functioning of the jet diffuser. Reduction of the maximum pressure gradient could be accomplished by a choice of larger values of *b,* but this would result in longer diffusers and was considered undesirable. Instead, the values of *da, db,* and *dc* were systematically varied in an attempt to improve the performance while avoiding any increase of the diffuser length.

The results of this analysis are described in Fig. 8, where it is shown that increases of *da* provide smaller maximum pressure gradients, and although not shown, they provide smaller differences between maximum pressure gradients among streamlines, a small change in the distribution of β_0 and a small increase of diffuser length compared to configuration A. Larger increases of *da* (greater than 1.905 cm) resulted in a more rapid increase of diffuser length with decreasing pressure gradients. Increasing *db* while $da = dc = 0$ produced an effect similar to that of decreasing *b,* but the increase of maximum pressure gradient with decrease of the maximum diffuser length is slower than that of decreasing *b,* and provides better peripheral pressure distribution. Increasing *dc* while $da = db = 0$ provided a decrease in the maximum pressure gradient and in the diffuser length as indicated in Fig. 8; however, the initial flow angle (β_0), near the ejector end, increased rapidly with increasing values of *dc.*

A repetition of the above analysis for $b = 9.525$ cm produced the results depicted also in Fig. 8. The essential aspect of these results consists of the observation that the knee of the curve lies closer to $da = 0$ as *b* decreases. It was therefore evident that an increase of *b* to values greater than 10.160 cm would permit the use of larger values of *da* and *db* before reaching the knee of the curve, thus providing a means for large reduction of the maximum pressure gradient and a

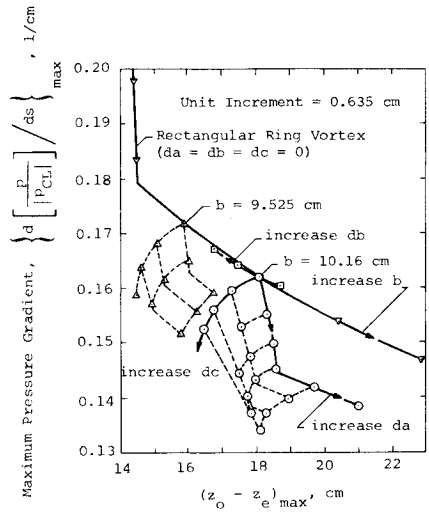

Fig. 8 Maximum pressure gradient vs maximum diffuser length for constant exit angle.

decrease of the peripheral pressure gradients. Further, increases of *dc* were utilized to avoid excessive lengthening of the diffuser. Using this information, and increasing the exit angle of the diffuser (β_e) at the middle plane to 50 deg, a second diffuser (configuration B) was designed.

The parameters of this diffuser are as follows:

$$b = 10.7950 \text{ cm} \qquad da = 4.4450 \text{ cm}$$

$$db = 0.9525 \text{ cm} \qquad dc = 0.7620 \text{ cm}$$

and the boundary conditions are

$$\beta_0 = 9.61 \text{ deg} \qquad \beta_e = 50 \text{ deg at } 2x_e/X_2 = 2.5$$

These conditions determined the values of *a* and *c* to be as follows:

$$a = 13.5930 \text{ cm} \qquad c = 1.2499 \text{ cm}$$

The maintenance of a fixed value of β_e for all streamlines results in a nonuniform length $(z_0 - z_e)$. Practical considerations however require termination of the diffuser at a constant length along its periphery. A cutoff of the configuration A diffuser at a constant length $(z_0 - z_e) = 13.5$ cm was tested with virtually no adverse effect. Thus the diffuser (configuration B) was cut off at a length of 12.7 cm from the diffuser jet slot, resulting in a nonuniform distribution of β_e. In addition, the diffuser jet slot thickness (t_d) was enlarged at the corners to achieve a reasonably uniform diffuser jet thickness at the end of the solid surface, in view of the larger surface divergence and higher maximum pressure gradient encountered by stream tubes near the corners. Figure 9 displays the characteristics of the configuration B diffuser in comparison to those of configuration A cut off at 13.5 cm from the diffuser jet slot.

The entire ejector assembly with configuration B diffuser is illustrated in Fig. 10. The shape of the configuration B diffuser is also illustrated in this figure, with contour lines at a spacing of 1.27 cm. As shown in Fig. 11, the thrust augmentation of this ejector exceeded 2.13 with a diffuser length/throat width equal to 1.4, and an inlet area ratio, $A_2/(s_\infty + a_\infty)$ of 21.

It is estimated (by the methods described in Ref. 1) that when high pressure energized gas is injected as primary fluid, as in the case of V/STOL applications, the optimal diffuser area ratio is smaller than that required at lower pressures. For example, at a nozzle plenum pressure to ambient pressure ratio of 3, an AJDE energized by fan air, requires a diffuser

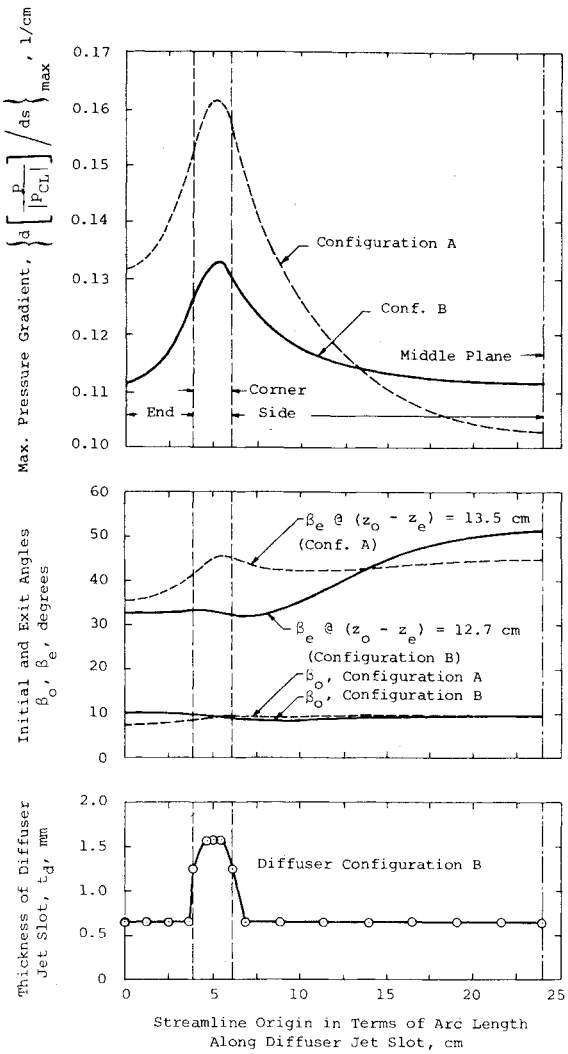

Fig. 9 Comparison of configurations A and B.

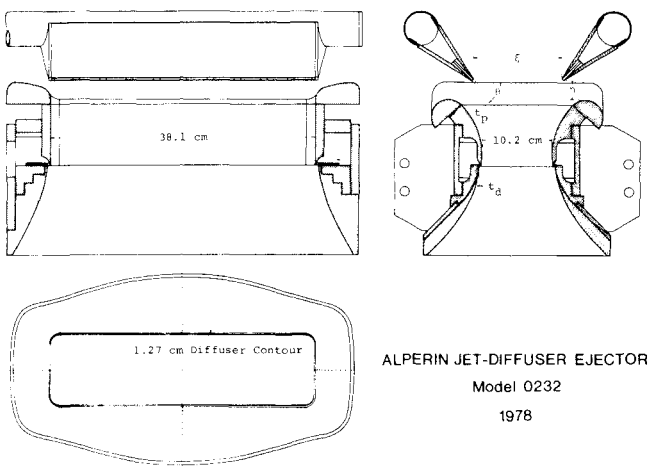

Fig. 10 AJDE with configuration B diffuser.

area ratio of about 2. This corresponds to a cutoff of configuration B diffuser at about 9.14 cm from the diffuser jet slot, and the diffuser length becomes smaller than the width of the ejector's throat.

The successful elimination of the large, protruding end plates previously used on the STAMP ejector, accompanied by superior performance, demonstrates the utility of the potential flow method for the design of the ejector surfaces.

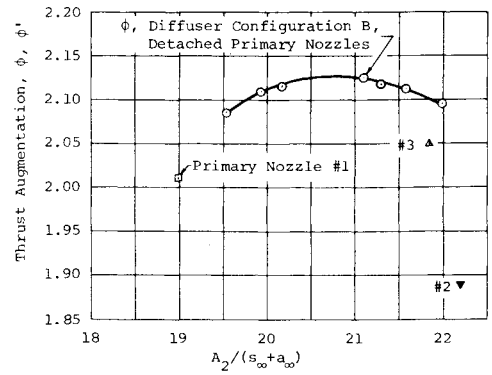

Fig. 11 Performance of configuration B diffuser with various primary nozzles.

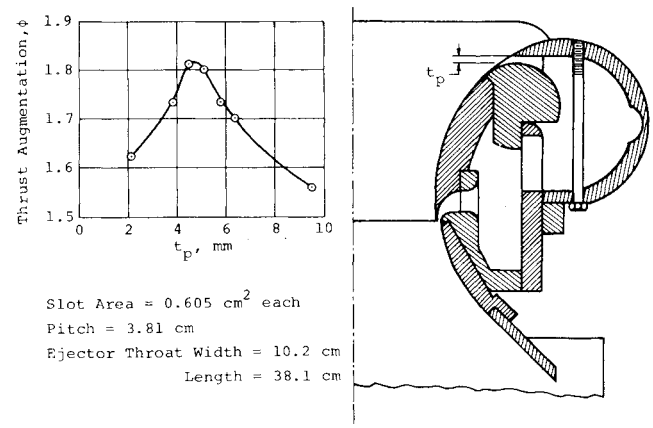

Fig. 12 Performance of AJDE with segmented attached primary nozzles.

III. Primary Nozzles

The detached, protruding primary nozzles utilized on the STAMP ejector, although suitable for that application, represent an integration difficulty when applied to a high speed aircraft for V/STOL maneuvering. Previous attempts to attach the nozzles to the inlet of the ejector, and to utilize the Coanda effect to direct the flow towards the thrust direction, resulted in serious penalties in performance, owing to the large losses attributable to the skin friction on the inlet surfaces. To reduce these losses, the primary nozzles with continuous slots were replaced by rectangularly segmented slot nozzles as illustrated on Fig. 12.

The primary slot thickness (t_p) was varied over a range from 2.1 to 9.5 mm, maintaining a constant slot area of 0.605 cm^2, or since the ejector's throat is 10.2 cm wide and 38.1 cm long, and since there were ten slots per side, the ratio of throat area to nozzle area was about 32. With a fixed diffuser jet area and local and viscous flow effects, this corresponds to an overall inlet area ratio $A_2/(s_\infty + a_\infty)$ of 21, as determined from measurements of mass flow rate and plenum conditions in both the primary and diffuser jet flows. This arrangement, tested at a plenum pressure of 24.1 kPa (gage) (3.5 psig) produced an ejector performance as shown in Fig. 12. The thrust augmentation increased to a value of 1.82 as the slot thickness increased from 2.1 to about 4.4 mm, and decreased rapidly as the slot thickness was further increased. The rational for this behavior follows.

Since for a fixed diffuser design, thrust augmentation is improved by mixing and is adversely affected by friction, the smaller slot thicknesses create more contact surface between the primary jet and the ejector surface and result in an adverse influence due to skin friction. The rapid turning of these thin jet sheets also prevent effective mixing. As the slot thickness is increased, the skin friction becomes less predominant, the

Table 1 Adjustable primary nozzles

Primary nozzle				Maximum performance (experiment)				Induced flow	
No.	Spacing, cm	i.d., cm	o.d., cm	θ, deg	ϕ'	x, cm	z, cm	$1-\psi/\psi_w$	ω, deg
1	3.81	0.940	1.270	55	2.01	7.6	10.4	0.30	57.7
				60	2.00	7.1	10.2	0.33	59.4
				65	1.98	6.6	10.2	0.37	61.0
2	6.35	1.092	1.270	55	1.89	8.4	10.7	0.27	55.2
3	2.54	0.704	0.953	50	1.99	7.4	10.9	0.35	57.9
				55	2.03	6.4	10.2	0.39	61.7
				60	2.05	6.4	10.2	0.39	61.7

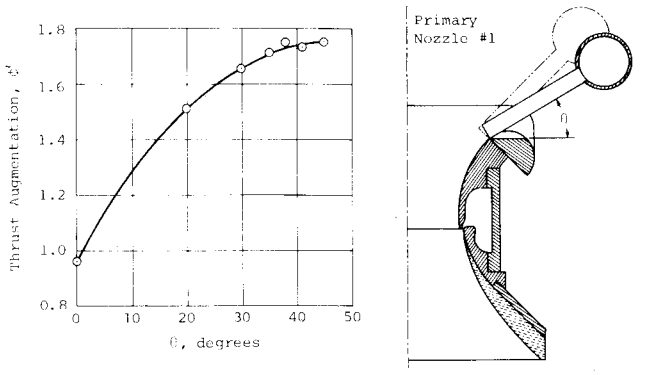

Fig. 13 Influence of primary jet orientation on thrust augmentation (near the wall).

turning less effective, and the mixing and performance are improved. Further increase of the slot thickness to values larger than 5.1 mm causes impingement of the flow from opposing primary nozzles upon each other, due to ineffective turning, resulting in momentum cancellation, creating a distorted flowfield which cannot entrain the surrounding fluid effectively, thus resulting in a corresponding decrease in thrust augmentation. Apparently, these factors indicate a requirement to inject the primary fluid at a position and at an angle which can avoid momentum cancellation while providing adequate mixing. To examine the influence of the position, orientation and spacing of the primary nozzles, three pairs of primary nozzles which were adjustable in position and orientation were designed, fabricated, and tested over a large range of positions and orientations. These nozzles were of circular cross section, 10.2 cm long and attached to a supply duct with a 5.1-cm o.d. The configuration of these three sets of adjustable primary nozzles are described in Table 1 and their appearance, mounted on the ejector is illustrated in Fig. 13.

Thrust augmentations reported for these adjustable nozzles (ϕ') were evaluated as the ratio of the total force on the ejector measured with load cells, to the thrust of a reference jet whose mass flow is equal to that of the injected gas and whose exit velocity is that resulting from an isentropic expansion from the plenum temperature and stagnation pressure measured at the center of a primary nozzle exit. It is estimated that this reference jet thrust is larger than the actual injected momentum, and therefore the data are conservative. Initially, the No. 1 nozzles were located immediately adjacent to the inlet surface and their angle was varied from 0 to 45 deg. The setup and results of this series of tests are shown in Fig. 13. As shown the maximum thrust augmentation was achieved at 45 deg; a slope which corresponds to the slope of the inlet surface at the nozzle location. Greater inclination of the nozzles will lead to impingement of the primary flow upon the inlet surface with the expected drop in performance.

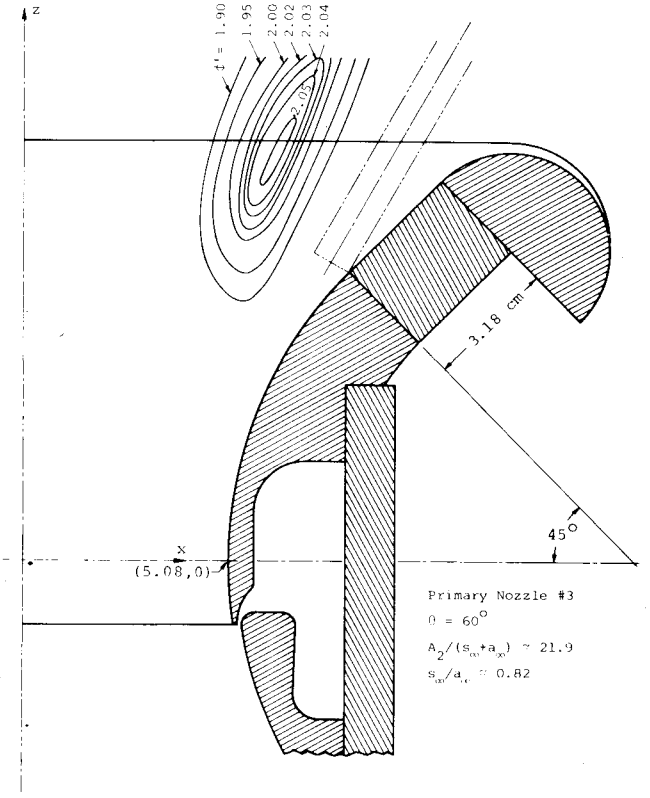

Fig. 14 Constant augmentation lines.

Tests performed with the nozzles separated from the surface utilized an extension of 3.81 cm, as illustrated in Fig. 14, to provide space for the eventual installation of the attached nozzles. The results of these tests were organized and mapped as constant augmentation lines on the ejector inlet area as illustrated by the example shown in Fig. 14. A distinct optimal point existed for each nozzle inclination, as illustrated. Since the ejector inlet is basically a two-dimensional design, the potential flow model described in Fig. 3 can be used to correlate the experimental results. For an ejector duct which consists of two identical cylindrical surfaces separated by a distance which corresponds to their radius of curvature, the stream function for the flow within the duct can be described as in Ref. 4;

$$\psi=\left(\frac{\Gamma}{4\pi}\right)\ell n\frac{z^2+(x-a)^2}{z^2+(x+a)^2}$$

where

$$a=\sqrt{5/4}X_2$$

and the local flow angle (defined similar to θ of Fig. 10 or 13)

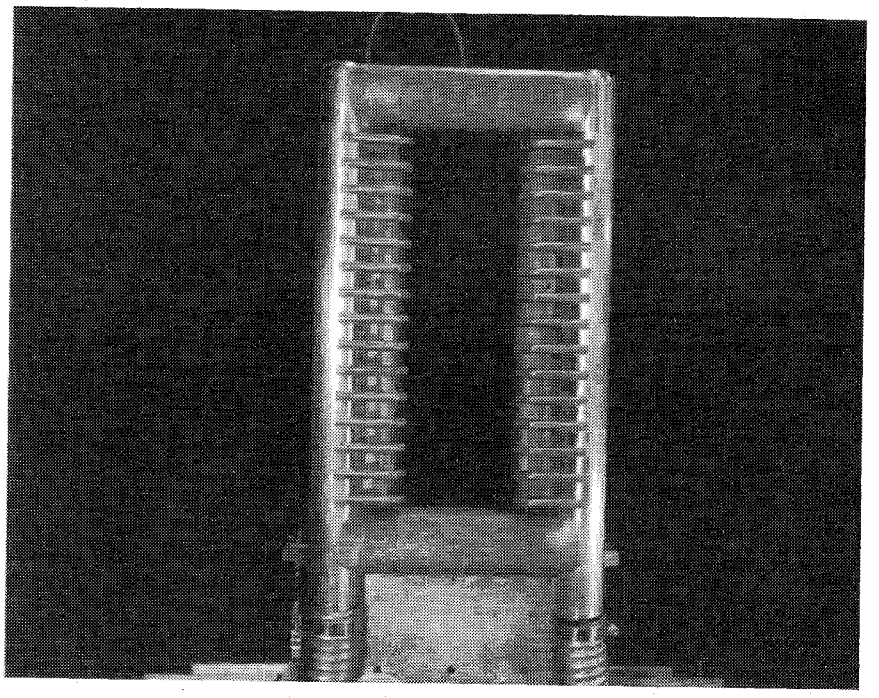

Fig. 15 Primary nozzle No. 4 on jet-diffuser ejector.

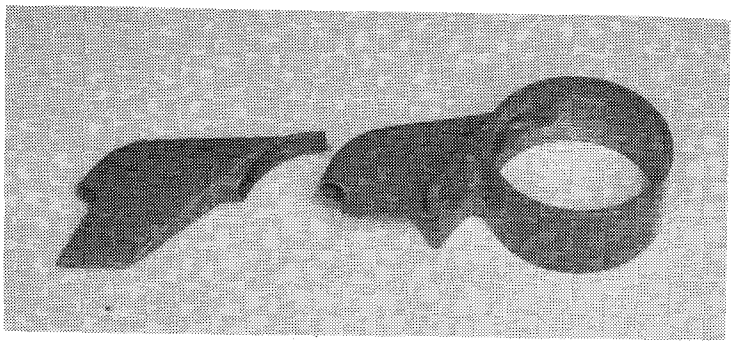

Fig. 16 Primary nozzle No. 4 mounted on supply duct and No. 4A showing extended fairing.

is expressed as

$$\omega = 90 \text{ deg} - \sin^{-1}\left[\left(\frac{z}{a}\right)\frac{1-\exp(4\pi\psi/\Gamma)}{1+\exp(4\pi\psi/\Gamma)}\right]$$

A summary of the test results (similar to Fig. 14) of the adjustable nozzles (Ref. 5) and a theoretical correlation of the induced flow derived from the two-dimensional potential flow are presented in Table 1.

It is important to point out that

1) $(1-\psi/\psi_w)$ is a measure of the amount of induced flow between the nozzle exit plane and the inlet surface, compared to the overall induced flow [since $\psi=0$ at the center line ($x=0$), the unsubscripted ψ refers to the stream function at the plane of the nozzles, and the subscript w is used to designate the stream function at the wall, or inlet surface]. To achieve optimal performance, this quantity is about one-third.

2) ω is the angle of the induced flow (calculated from the last equation with the coordinates given in Table 1) defined similarly to θ for comparison purposes. The best ejector performance occurs when ω is very close to θ. This means that attempts to accelerate mixing by creating vorticity of large strength (crossing primary and induced flow at large angles) may not be desirable.

As indicated in Table 1, nozzle Nos. 1 and 3 produced the largest thrust augmentations. The relatively low performance of nozzle No. 2 is attributed to its large spacing between nozzles and the large area of each individual jet, which may result in an inadequate mixing for this nozzle orientation. Although in designing these adjustable nozzles, an attempt was made to select the most suitable inlet area ratio $[A_2/(s_\infty + a_\infty)]$, for the configuration B diffuser, the use of standard tubing sizes precluded exact duplication of this characteristic. The result of this design consideration was indicated earlier in Fig. 11, where typical inlet area ratios achieved with each set of nozzles is shown plotted vs the maximum thrust augmentation achieved by each, and comparison is made with the data acquired with detached nozzles previously discussed.

Comparative evaluation of the above data and design considerations resulted in the selection of nozzle No. 3 at an exit coordinate of ($x=5.59$ cm and $z=8.44$ cm) with a 60-deg orientation and a corresponding $\phi' = 2.03$ as a design choice. Based upon this selection, a set of attached nozzles (No. 4) was designed, fabricated, and tested. The internal duct of these nozzles was of a continuously reducing cross-section elongated at the root while turning to a 60 deg inclination with a circular exit. The external fairing is a tapered NACA 4-digit airfoil. The nozzle configuration as it appears installed in the test article is illustrated on Fig. 15.

Testing of the No. 4 nozzles indicated a high internal flow efficiency, but exhibited an instability in the external (induced) flow, owing to separation from the external surfaces of the nozzles, precluding steady-state force measurement. To alleviate this instability, the chord length of the nozzle fairing was increased (No. 4A) as illustrated in Fig. 16.

With the extended, external fairing chord, the instability was eliminated and an increase of performance was observed. However, this set of nozzles had a maximum fairing thickness of 1.067 cm, which occupied 42% of the nozzle spacing, since the nozzles are 2.54 cm apart. This blockage resulted in some

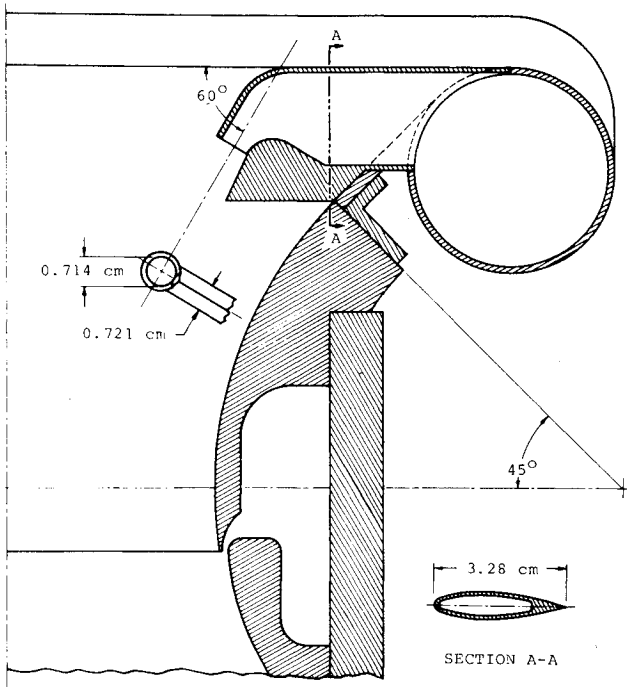

Fig. 17 Primary nozzle No. 5.

undesirable effects including 1) high induced flow loss due to blockage, 2) shifting of the best location of the nozzle exit owing to blockage near the inlet surface, and 3) sensitivity to large inlet disturbances.

Despite a measured thrust augmentation of 2.02, it appeared desirable to design one additional set of nozzles with reduced thickness and thickness ratio of the nozzle fairing. The internal duct was reshaped to conform to the external fairing shape while attempting to retain the high internal flow efficiency. This set of attached nozzles (No. 5) is illustrated in Fig. 17, and its basic dimensions, in comparison to those of Nos. 4 and 4A, are summarized in Table 2. The blockage reduction achieved by the nozzle No. 5 design, compared to nozzle 4A, significantly improved flow stability, but the improvement of performance was offset by increased internal losses as can be observed in the nozzle efficiency experiments described in Ref. 5. For most ejector applications, the Reynolds number of the primary nozzle flow is expected to be higher than that of the present experiment, and the performance penalty due to internal flow loss of the primary nozzles is expected to decrease. Therefore the more compact design of primary nozzle No. 5 is preferred to that of 4A.

Table 2 Attached nozzle properties

Nozzle	Maximum thickness t, cm	Maximum chord[a] c, cm	Typical t/c thrust direction	t/c at root flow direction	ϕ
4	1.067	3.284	0.325	0.230	...
4A	1.067	4.191	0.255	0.180	2.02
5	0.721	3.284	0.220	0.156	2.02

[a] Chord is measured in the thrust direction.

In summary, design of primary nozzles requires consideration of the

1) shape of nozzle discharge jet,
2) location and orientation of injected jet,
3) losses in internal flow of nozzle,
4) losses in external flow around nozzle,
5) interaction among 1, 2, and 4.

Acknowledgments

The information contained in this document was acquired as a result of contractual support from the Naval Weapons Center, China Lake, Calif., Bradley D. Kowalsky and James G. Martz III, project monitors; the Naval Air Development Center, Warminster, Pa., Dr. Ken Green, project monitor; and NASA Ames Research Center, Moffett Field, Calif., K. Aoyagi and Dave Koenig, project monitors.

References

[1] Alperin, M. and Wu, J.J., "High Speed Ejectors," Flight Dynamics Research Corp., AFFDL-TR-79-3048, May 1979.

[2] Alperin, M. and Wu, J.J., "Underwater Jet-Diffuser Ejector Propulsion, Real Fluid Effects," Flight Dynamics Research Corp., ONR Contract No. N00014-77-C-0294, FDRC 0294-8-78, Aug. 1978.

[3] Alperin, M., Wu, J.J., and Smith, C.A., "The Alperin Jet-Diffuser Ejector (AJDE) Development, Testing, and Performance Verification Report," Flight Dynamics Research Corp., Naval Weapons Center, NWC TP 5853, Feb. 1976.

[4] Alperin, M. and Wu, J.J., "End Wall and Corner Flow Improvements of the Rectangular Alperin Jet-Diffuser Ejector," Flight Dynamics Research Corp., Naval Air Development Center, NADC-77050-30, May 1978.

[5] Alperin, M., and Wu, J.J., "Jet-Diffuser Ejector—Attached Nozzle Design," NASA CR 152361, May 1980.